

WADC TECHNICAL REPORT 55-225

STRENGTH, DAMPING, AND ELASTICITY OF MATERIALS  
UNDER INCREASING REVERSED STRESS  
WITH REFERENCE TO ACCELERATED FATIGUE TESTING

F. H. VITOVEC  
and  
B. J. LAZAN  
UNIVERSITY OF MINNESOTA

JUNE 1955

Materials Laboratory  
Contract No. AF 33(038)-20840  
PROJECTS NO. 7360 and 3346  
TASKS NO. 73604 and 73498

Wright Air Development Center  
Air Research and Development Command  
United States Air Force  
Wright-Patterson Air Force Base, Ohio

## FOREWORD

This report was prepared by the University of Minnesota, under USAF Contract No. AF33(038)-20840 and covers work during the period of January 1953 to December 1954. The USAF Contract was initiated under Project No. 7360, "Materials Analysis and Evaluation Techniques", Task No. 73604, "Fatigue Properties of Structural Materials", formerly RDO No. 614-16, and Project No. 3346, "Propeller Blades", Task No. 73498, "Evaluation of Accelerated Fatigue Testing Procedures", formerly RDO No. 591-80. The contract was administered under the direction of the Materials Laboratory, Directorate of Research, Wright Air Development Center, with Mr. W. J. Trapp acting as project engineer.

In addition to the authors, the following personnel of the University of Minnesota contributed to this work: N. Foker and F. Abigt served as technicians, H. Binder was responsible for the metallographic work, R. Ruegemer and J. Whittier plotted the diagrams. Drafting work and manuscript preparation were by M. Chapin, B. Gulbrandson, D. Schultz, and H. Thomas.

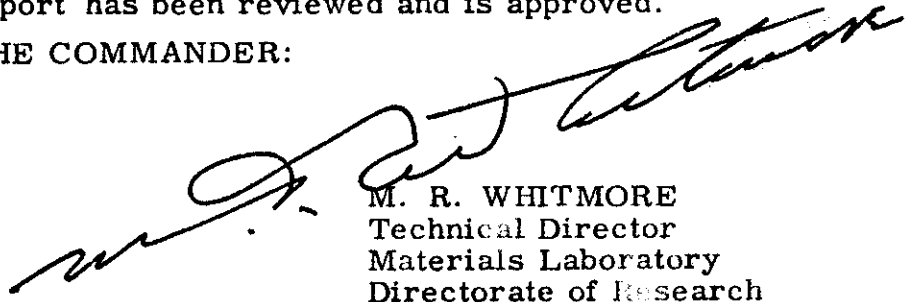
## ABSTRACT

The purpose of the work was to investigate the damping, stress-strain, and failure properties under uniformly increasing stress amplitude and to determine the relation of these properties to conventionally determined fatigue strength. Data are presented on SAE 1020 Steel, 24S-T4 Aluminum Alloy, SAE 4340 Steel, and RC-55 Titanium under rotating bending stress amplitudes which (a) are progressively increased during the test and (b) are held constant as in conventional fatigue tests. The Gough dynamic proportional limit method and the Lehr damping intercept under uniformly increasing stress amplitude were found to agree with the conventional fatigue strength only for certain materials and to be misleading in other cases. The failure stress at different rates of stress increase and different starting stresses was determined to evaluate the reliability of the Prot short-time fatigue testing method. For the materials tested Prot starting stress below the cyclic stress sensitivity limit (in the region where damping is unchanged by stress history) has practically no effect on the Prot failure stress. In general, the test results for the four materials indicate that the Prot method indicates the conventional fatigue strength with a reliability of 10 per cent. The use of modified Prot methods which utilize exponents other than 0.5 were not significantly better for indicating fatigue strength.

## PUBLICATION REVIEW

This report has been reviewed and is approved.

FOR THE COMMANDER:



M. R. WHITMORE  
Technical Director  
Materials Laboratory  
Directorate of Research

## TABLE OF CONTENTS

Section		Page
I	Introduction . . . . .	1
II	Objectives, Procedures, and Test Program . . . . .	2
III	Test Materials and Specimen Preparation . . . . .	3
IV	Testing Machine and Test Procedure . . . . .	3
V	Fatigue and Damping Properties Under Constant Stress Amplitude . . . . .	4
VI	Fatigue Strength Under Progressive Load Increase . . . . .	5
VII	Damping Properties Under Progressive Load Increase and Lehr's Method . . . . .	6
VIII	Effect of Fatigue on Stress-Strain Properties and Gough's Dynamic Proportional Limit Method . . . . .	7
IX	Summary and Conclusions . . . . .	8
	Bibliography . . . . .	10

## LIST OF TABLES

Table		Page
I	Test Materials and Data . . . . .	12
II	Fatigue Test Data for SAE 1020 Steel at Various Loading Rates and Different Initial Stresses . . . . .	13
III	Fatigue Test Data for 2024-T4 Aluminum Alloy at Various Loading Rates and Different Initial Stresses . . . . .	15
IV	Fatigue Test Data for SAE 4340 Steel at Various Loading Rates . . . . .	16
V	Fatigue Test Data for RC-55 Titanium at Various Loading Rates and Different Initial Stresses . . . . .	17

## LIST OF FIGURES

Figure		
1	Photomicrographs of Test Materials in Testing Condition . . . . .	19
2	Rotating Cantilever Beam Fatigue and Damping Test Machine with Variable Speed Transmission for Progressive Load Increase Tests . . . . .	20
3	S-N Fatigue Diagrams of Test Materials . . . . .	21
4	Comparison of the Effect of Cyclic Stress of Several Magnitudes on the Total Damping Energy of Test Materials . . . . .	22

5	Total Damping Energy of Test Specimen Under Both Constant and Progressively Increasing Stress Amplitude as a Function of Stress for Various Stress Histories . . . . .	23
6	S-N Curves Obtained Under (a) Constant Stress Amplitude Conventional Tests and (b) Uniformly Increasing Stress Amplitude. Cycles Plotted are Those Above Highest Starting Stress . . . . .	24
7	N Versus ( $S-S_e$ ) Diagram for Determination of the Constants in Weibull's Equation . . . . .	25
8	Failure Stress Under Progressive Load Increase as a Function of Loading Rate $\alpha$ to the Various Values of Power n for SAE 1020 Steel . . . . .	26
9	Failure Stress Under Progressive Load Increase as a Function of Loading Rate $\alpha$ to the Various Values of Power n for 2024-T4 Aluminum Alloy . . . . .	27
10	Failure Stress Under Progressive Load Increase as a Function of Loading Rate $\alpha$ to the Various Values of Power n for SAE 4340 Steel . . . . .	28
11	Failure Stress Under Progressive Load Increase as a Function of Loading Rate $\alpha$ to the Various Values of Power n for RC-55 . . . . .	29
12	Linear Plot of Damping Energy Versus Alternating Stress at Different Loading Rates for SAE 1020 and RC-55 Titanium . . . . .	30
13	Deviation from Stress-Strain Linearity as a Function of Amplitude of Reversed Stress and Various Loading Rates for SAE 1020 and SAE 4340 Steel . . . . .	31
14	Deviation from Stress-Strain Linearity as a Function of Amplitude of Reversed Stress, Loading Rate, and Starting Stress for RC-55 Titanium . . . . .	32

*Contrails*

## STRENGTH, DAMPING, AND ELASTICITY OF MATERIALS UNDER INCREASING REVERSED STRESS WITH REFERENCE TO ACCELERATED FATIGUE TESTING

### SECTION 1. INTRODUCTION

The determination of the fatigue properties by the conventional Woehler Method under constant stress amplitude may be very time consuming. Not only is it necessary to carry some specimens to large number of cycles, but also large numbers of specimens are sometimes required for statistically sound conclusions.

In view of the importance of reducing fatigue testing time, there has been considerable interest for over forty years in accelerated fatigue testing methods (1).<sup>1/</sup> Most of the methods are based on the relationship between the fatigue strength and other physical properties of the material. The several methods investigated from 1920 to 1930 indicated that reliable results could be expected under certain conditions. Since some methods were useful only for certain materials and others could do no more than provide comparative results, interest in short-time fatigue testing methods decreased. Recently, however, Prot (2) proposed a new method which has renewed interest in accelerated test methods.

Whereas in the conventional fatigue test the load or strain amplitude is maintained constant until fatigue failure occurs, in the progressive load increase (or Prot method) the load amplitude is uniformly increased until failure occurs. The rate of load increase is maintained constant during a given test, but may be different for different tests. In the Prot approach the mean value of the failure stress at each rate of load is plotted against the square root of the loading rate and the fatigue limit is presumably obtained by extrapolating a straight line through these points to zero loading rate. In order to save time, Prot recommended starting the test at a stress approximately 6,000 psi below the expected fatigue strength.

Prot based his method on the assumption that the S-N curve is a hyperbola which is asymptotic to the fatigue limit (3); thus,

$$N = K (S - S_e)^m \quad (1)$$

where N is cycles to failure, S is reversed stress,  $S_e$  is the fatigue limit, and K and m are material constants. Prot further assumed that the damage per cycle is proportional to the difference between the test stress and the fatigue strength. This difference increases with the number of cycles under progressive load increase leading to failure stresses which lay on another hyperbola with the fatigue strength as the horizontal asymptote. This assumed relationship indicates that the failure stress under uniform load increase is a linear function of the square root of the loading rate. Thus;

$$S_R = S_e + K \sqrt{\alpha} \quad (2)$$

where  $S_R$  is the failure stress corresponding to the particular loading rate  $\alpha$  in psi per cycle.

The interpretation of test results obtained from progressive load increase tests is not as simple as proposed by Prot since the effect of under-stressing (4) and of the non-linearity of damage with respect to specimen life (5) must often be considered. Therefore, the Prot failure stress is not always a linear function of the square root of the loading rate as discussed above.

---

<sup>1/</sup> Numerals in parentheses refer to references in the Bibliography.

D. L. Henry (6) investigated the problem of failure under progressive load increase by using Miner's type of criterion for cumulative damage in fatigue (7). Modified so that the sum of damage increments reach a value which may be different from unity. Like Prot, Henry used hyperbolic approximations for the conventional S-N curve and found that:

$$S_R = S_e + D \alpha^n \quad (3)$$

for

$$n = \frac{1}{m+1} \quad (4)$$

In Henry's method the exponent  $n$  is determined from the constant  $m$  associated with the conventional S-N curve (see Equation 4) while Prot assumed that  $n$  is 0.5 independent of the S-N curve.

The reliability of Prot's short-time fatigue testing method was the subject of several investigations, (8) through (12). In general, it is found that Prot's method gives a good indication of the conventionally determined fatigue strength for ferrous alloys with a well-defined fatigue limit. However, for nonferrous metals, such as aluminum alloys, the value of exponent  $n$  in Equation (3) which fits the experimental data best may differ considerably from the conventionally determined one.

In Prot's earlier work he recommended starting the progressive load increase test approximately 6000 psi below the expected fatigue limit. Corten, Dimoff, and Dolan (11) investigated the effect of starting stress on the fatigue strength determined by the Prot method and found that in general, lower starting stresses resulted in a slightly lower value of the Prot fatigue strength. However, this work indicates that the effect of starting stress also depends on the type of material and its condition, being larger for metals "susceptible to coxing", in this case resulting in higher values of the Prot fatigue strength.

Several other short-time fatigue testing methods based on properties under uniformly increasing alternating load have also been proposed (1). Among these are Gough's dynamic proportional limit criterion (13) and Lehr's damping intercept criterion (14).

In view of the conflicting observations made regarding the reliability of these three short-time methods for determining the fatigue strength from the progressive loading increase tests, the additional work described below was undertaken.

## SECTION II. OBJECTIVES, PROCEDURES, AND TEST PROGRAM

The purpose of this program was to investigate the reliability of various progressive load increase methods for determining fatigue strength. Rotating beam tests were used for this purpose so that the following three properties could be conveniently measured under uniformly increasing stress: (a) damping energy, (b) dynamic modulus of elasticity, and (c) failure stress. The damping properties were procured to check the reliability of Lehr's damping intercept criterion, the elasticity data were intended to check Gough's dynamic proportional limit method, and the failure stress data were determined to check the Prot approach.

In order to help clarify understressing and damage effects, various starting stresses were used. Progressive load increase tests were started at zero stress, near the cyclic stress sensitivity limit\* for damping (15) and between this limit and the fatigue strength. For each starting stress, tests were performed under three different loading rates.

---

\* See section on "Results and Discussion" for definition of the cyclic stress sensitivity limit.



Two ferrous and two nonferrous materials were used to cover a range of material types and provide a more critical check on reliability of conclusions. The materials used, starting stress, loading rate, and other details of the test program are given in Table I.

Conventional fatigue tests under constant stress amplitude were also performed for comparison purposes. The damping and modulus properties were also determined during these conventional fatigue tests.

## SECTION III. TEST MATERIALS AND SPECIMEN PREPARATION

The test materials used in this investigation were SAE 1020 steel, 2024-T4 aluminum alloy, SAE 4340 steel, and RC-55 titanium. The chemical analysis, treatment and test condition, and the mechanical properties of the test materials are listed in Table I. Photomicrographs of the materials in test condition are shown in Figure 1.

The specimens used in this work were of circular cross section and slightly tapered to produce uniform stress along the test length under the cantilever beam loading used. The length of the tapered test section was 1.75 inch, with  $\frac{1}{4}$  inch fillet radius on each end. The specimen diameters are listed in Table I.

The test specimens were rough turned, using water and oil coolant, from 0.05 to 0.01 inch oversize at a speed of 325 rpm, a feed of 0.0042 inch per revolution, and a tool advance of 0.025 inch. Finish turning was from 0.003 to 0.005 inch oversize for the 4340 and titanium specimens under conditions similar to rough turning except for a 0.075 to 0.003 inch tool advance and a lower speed (45 rpm for the titanium). The SAE 1020 steel and 2024-T4 aluminum specimens were left 0.02 inch oversize, then ground to 0.002 inch oversize with 120 - 06 - V10 Aloxite wheel with a feed of 0.0015 inch per revolution using Tycol-Afton 8 coolant. All specimens were finally polished using silicon carbide sanding belts, the final passes being with a belt having a grit size from 400 to 900. For the SAE 4340 specimens kerosene coolant was used during final polishing and  $\text{CO}_2$  was used for the titanium.

All materials were thermally treated before machining except that the 4340 steel was rough machined to 0.01 inch oversize, then heat treated, and finally finish machined and polished.

## SECTION IV. TESTING MACHINE AND TEST PROCEDURE

The rotating cantilever beam fatigue, damping, and elasticity testing machine used in this work has been described previously (16). For the progressive load increase tests, the machine was adapted with a variable speed transmission between the main motor and the table angle adjuster so that the desired rate of load increase could be applied to the test specimen. A photograph of the adapted machine is shown in Figure 2. The variable ratio transmission T is driven by motor M which rotates the fatigue specimen S, so that the psi per cycle increase during a progressive load increase test is independent of the frequency of stress on the specimen.

All the tests were performed at room temperature. The testing speed was 1000 rpm for 2024-T4 aluminum alloy and RC-55 titanium and 2000 rpm for SAE 1020 and SAE 4340 steel. In all cases the frequency of cyclic stress during damping and deflection readings was 20 rpm.

Conventional fatigue tests under constant stress amplitude were performed with the same type of testing machine and specimen as the progressive load increase tests.

## SECTION V. FATIGUE AND DAMPING PROPERTIES UNDER CONSTANT STRESS AMPLITUDE

The S-N fatigue data procured under conventional constant stress amplitude conditions are listed in Tables 2, 3, 4, and 5, and plotted in Figure 3.

During the course of each constant stress amplitude fatigue test, the damping energy absorbed by the test specimen was continuously determined. Typical data procured for the four test materials are shown in Figure 4. Observe first in Figure 4 that under relatively low stress, the damping does not change with stress history (that is, number of stress cycles) but as the stress approaches the fatigue strength then damping is affected by repeated fatigue stress. The four test materials diagramed showed different patterns of change during sustained cyclic stress; for example, the titanium and mild steel increase in damping with stress history, whereas the aluminum alloy decreases up to immediately before failure. However although the pattern of change at high stress amplitudes is different for different materials, it should be observed that all test materials have one behavior in common; damping does not change with number of cycles at low and intermediate stress amplitudes but is affected by sustained cyclic stress near and above the fatigue limit. <sup>1/</sup>

The stress history dependence of damping can better be seen in Figure 5 which shows damping versus stress amplitude on a log-log basis. The stress history effects at high stress amplitude are shown in these diagrams by the family of curves for each material. For example, the curves labeled  $10^{1.3}$  indicate the damping after 20 cycles. Although these curves for the four different materials are quite dissimilar in many respects, they all display a "cyclic stress sensitivity limit" SL (see solid square dots). Below this limit the log-log plot of damping versus stress curve is a single valued curve, usually a straight line, indicating no stress history effect. Above this limit, however, two changes generally occur. First the damping becomes not only a function of stress amplitude, but also of number of prior stress cycles and thus a separate curve is required for each stress history. Secondly, a change in the slope generally occurs, in some cases quite abruptly. For the four materials under discussion, the cyclic stress sensitivity limit varies between 60 and 88 per cent of the fatigue strength at  $2 \times 10^7$  cycles. The existence of a cyclic stress sensitivity limit has been observed not only in the four alloys under discussion, but in over ten others investigated to date, some at elevated temperatures (15).

In some materials, mild steel for example, both the change in slope and the effect of stress history on damping occur abruptly at a definite stress and the cyclic stress sensitivity limit is well defined. In other materials, such as in the aluminum alloy, these changes are much more gradual and the point defined as the stress sensitivity limit depends on the sensitivity of measurements. In this regard the difficulties in defining the cyclic stress sensitivity limit are similar to those encountered in defining a proportional limit under static stress.

The effect of stress history on the damping properties seems to be associated with localized plastic deformation. In polycrystalline materials, some grains which are favorably oriented and are in a critical stress condition yield plastically, preferentially near the surface (17) at stresses which are significantly below the overall fatigue strength. However, the per cent volume of those grains is very small and their effect may be lost in the general overall observation. With increasing stress beyond the cyclic stress sensitivity limit the number of grains which yield plastically increases, slowly at first

<sup>1/</sup> This observation has been made for numerous other materials (15). However, it should be mentioned that RC-55 behaved rather erratically and did give some evidence of stress history effect at low stress amplitudes.

but with increasing rapidity. At stresses above the fatigue limit the per cent volume displaying significant plastic behavior is large enough to cause the gross effects observed.

Since damping is an extremely structure sensitive property, it appears reasonable to inquire about the relationship between the cyclic stress sensitivity limit and the stress below which fatigue coxing or damage becomes insignificant. One might expect that since cyclic stress below the stress sensitivity limit has little effect on damping, correspondingly it should also have little effect on subsequent fatigue strength at higher stress levels. However, cyclic stress above this limit changes the material significantly, as indicated by the change in damping. It might therefore be expected that these changes would be reflected as fatigue coxing or damage effects which might affect the fatigue life during subsequent loading at higher stress levels. Therefore, starting stresses both below and above this limit were used for some materials in the progressive load increase work described later.

## SECTION VI. FATIGUE STRENGTH UNDER PROGRESSIVE LOAD INCREASE

The fatigue strength test data procured under progressive load increase are listed in Tables 2, 3, 4, and 5, and plotted in Figure 6. Different starting stresses were used in order to determine their effect on failure strength, and also to clarify the relationship of coxing and fatigue damage to the cyclic stress sensitivity limit.

Considering first the mild steel, the upper part of Figure 6 shows the Prot failure stress determined at the different starting stress of 0, 29,000, 33,000, and 37,000 psi for different loading rates. The cycles to failure plotted for all curves are those imposed beyond the stress of 37,000 psi so direct comparison can be made for different starting stresses. Observe first that starting stresses of zero and 29,000 psi have about the same Prot failure stress, indicating little coxing or fatigue damage effect below the cyclic stress sensitivity limit. However if the starting stress is 33,000 or 37,000 psi, the curves are significantly below those for the lower starting stress. This indicates that at stresses between 29,000 and 33,000 psi, and between 33,000 psi and 37,000 psi there is sufficient coxing effect to produce the significant spread in the curves shown. For example, at a Prot loading rate of approximately 0.025 psi per cycle the fatigue failure stresses for different starting stresses were: 47,200 and 46,300 psi (average 46,700 psi) at 0 psi starting stress; 47,000, 46,600, 46,400, and 46,500 psi (average 46,600 psi) at 29,000 psi starting stress; 45,100, 44,700, and 44,000 psi (average 44,600 psi) at 33,000 psi starting stress; and 43,700, and 43,700 psi at 37,000 psi starting stress. The specimens started at zero and 29,000 psi failed at a higher stress than those started at 33,000 psi (failure stress 46,000 compared to 44,600 psi) apparently due to coxing effects between 29,000 psi and 33,000 psi even though the fatigue limit is at 35,000 psi. Similarly, stress history between 33,000 and 37,000 psi produced sufficient coxing effect (or a combination of coxing and damage) to account for the difference between the failure stress of 43,700 and 44,600 psi. Since the cyclic stress sensitivity limit is 29,000 psi it appears that this limit indicates the stress below which no coxing or fatigue damage effects occur but above which these effects may be significant in mild steel.

In the case of 2024-T4 aluminum alloy, diagramed in Figure 6, whether the test is started at 0 or 24,000 psi appears to make little difference in the Prot failure stress if cycles are counted beyond 24,000 psi in both cases. Since 24,000 psi is the cyclic stress sensitivity limit for this alloy, this limit appears to be the stress below which coxing or fatigue damage are insignificant.

For the case of the RC-55 Titanium shown in Figure 6, the starting stress effects appear to be too small to be separable from the scatter in the data. If there are coxing effects beyond the cyclic stress sensitivity limit of 24,000 psi, these are smaller than the scatter in the present data, and therefore no conclusions are possible at this time. In general the RC-55 data were more variable than for the other test materials.

In order to evaluate the reliability of Henry's modification of the Prot theory, the material constant  $m$  for each of the four test materials was determined as shown in Figure 7. This constant  $m$  was then used to compute the value of exponent  $n$  in accordance with Equation 4. In the Prot type diagrams which follow, these computed values of  $n$  as well as others are used for comparison purposes.

The Prot type diagrams shown in Figures 8, 9, 10, and 11 are intended to compare the effects of different values of  $n$  and starting stress. In each case, three values of  $n$  are plotted, (a)  $n_p$ , the 0.5 value originally suggested by Prot, (b)  $n_s$ , the value of  $n$  which results in the straightest line for failure stress, and (c)  $n_m$ , the value of  $n$  determined from the constant  $m$  for the material.

For mild steel, aluminum alloy, and titanium the plot failure stress under progressive load increase versus the square root of the loading rate ( $n_p = 0.5$ ) does not result in a straight line. However, if a straight line is approximated through these points the Prot fatigue strength so determined is in all cases within  $\pm 10$  per cent of the conventionally determined fatigue strength. For 4340 the Prot method provides a better approximation of the conventional fatigue strength, the difference being only 4%.

If the Prot test data are plotted according to exponent  $n_s$  of the loading rate which results in the straightest line the fatigue strength so determined is in some cases considerably smaller than the conventionally determined fatigue strength, as shown by RC-55 titanium, Figure 11.

The  $n_m$  values determined by Equation (4) from the constant  $m$  of the material differ in most cases from the two other values of  $n$ . In most cases  $n_m$  was different from the other values of  $n$  and appeared to offer no advantage. Theoretically the  $n_m$  value should produce straight line relationship, but since this is not generally the case, the validity of Miner's criterion that damage is a linear function of the number of cycles at a given stress should be questioned.

## SECTION VII. DAMPING PROPERTIES UNDER PROGRESSIVE LOAD INCREASE AND LEHR'S METHOD

Figure 5 shows damping energy versus stress amplitude considering both the constant stress amplitude and uniformly increasing stress tests.

The damping data of the SAE 1020 steel specimens indicate a cyclic stress sensitivity limit at 29,000 psi which is 83 per cent of the fatigue limit. Damping curves under progressively increasing stress, plotted in the same diagram, show a sharp break at this cyclic stress sensitivity limit. There seems to be no effect of loading rate on the damping behavior for starting stresses up to the cyclic stress sensitivity limit. For starting stresses above this limit damping increases more rapidly with increasing stress, as would be expected from stress history effects.

Fatigue tests at constant stress amplitude on 2024-T4 aluminum alloy show a cyclic stress sensitivity limit at approximately 25,000 psi, which is 89 per cent of the fatigue strength. However, damping curves during progressive load increase exhibit no such limit, the double logarithmic plot of damping versus stress being linear up to the failure stress. This also would be expected from the nature of the stress history effect.



SAE 4340 steel exhibits a cyclic stress sensitivity limit at approximately 55,000 psi which is 15 per cent below the fatigue strength. The damping data under progressive load increase fall within the history band of the data obtained under constant stress amplitude.

The diagram for RC-55 titanium indicates that considerable history effects occur at stresses below the fatigue strength. In view of scatter in the data the general trends are not conclusive. It is thus apparent from the above discussion that the damping versus stress relationship is very dependent on prior loading history.

In the short-time testing method suggested by Lehr (14) damping energy is plotted versus alternating stress to a linear scale. Lehr uses two different stresses as reference points, one which marks the beginning of the deviation of the curve from an approximate straight line in the low stress damping range, and a second which is obtained from the abscissa intercept of a line drawn tangent to the higher damping region of the damping stress curve. According to Lehr, the fatigue strength is near the lower stress limit for materials with a small initial damping, and near the higher stress limit for materials with a high initial damping. Considering what is now known regarding the nature of the damping versus stress relationship (15), the Lehr approach must be considered a rough approximation at best.

Figure 12 shows a linear plot of the damping energy-stress curve for SAE 1020 steel and RC-55 titanium. The diagrams for the steel and the location of the fatigue limit are in agreement with those published by Lehr. The diagram for titanium indicates a significant effect of the loading rate on the fatigue strength determined by Lehr's method. The highest loading rate, 0.09 psi per cycle, indicates a fatigue strength which is only one per cent smaller than the conventionally determined fatigue strength, but at other loading rates there is considerable difference. For the aluminum alloy Lehr's method cannot be applied since the change of damping is so gradual and no significant transition range can be observed. In the case of SAE 4340 steel the scatter of data was too large for use of the Lehr method.

In view of the stress history effects discussed above, the significance of the Lehr intercept method for determining the fatigue limit is very questionable.

## SECTION VIII. EFFECT OF FATIGUE ON STRESS-STRAIN PROPERTIES AND GOUGH'S DYNAMIC PROPORTIONAL LIMIT METHOD

H. J. Gough (13) determined a dynamic proportional limit under reversed cyclic stress by measuring alternating strain during progressively increasing alternating stress. He found a linear stress-strain relationship below a certain stress, beyond which the strains increase more rapidly than the stresses. He suggested that this dynamic proportional limit is a good indication of the fatigue strength.

In order to show the proportional limit more clearly, the deviation from stress-strain linearity rather than total strain (elastic plus plastic) was plotted as a function of amplitude of reversed stress in Figure 13. For the SAE 1020 steel specimens, the static proportional limit under bending stress was found at 41,000 psi. The dynamic stress-strain behavior depends on the loading rate and as shown in Figure 13, varies between 28,000 and 31,000 psi, increasing with increasing loading rate. The dynamic proportional limit averages 29,000 psi which is approximately 8 per cent smaller than the fatigue limit. It is interesting to note that the dynamic proportional limit of mild steel is of the same magnitude as the cyclic stress sensitivity limit.

Figure 13 shows also the deviation from stress-strain linearity as a function of amplitude of reversed stress for SAE 4340 steel. The diagram indicates that the dynamic proportional limit is a function of loading rate, decreasing with decreasing loading rate. The dynamic proportional limit under 0.09 psi per cycle loading rate is equal to the fatigue limit of this material, but is different at other loading rates.

Figure 14 shows the deviation from stress-strain linearity as a function of amplitude of reversed stress, loading rate, and starting stress for RC-55 titanium. The behavior of this material is rather unusual as explained previously. Both the static and dynamic proportional limit are smaller than the fatigue strength, in fact, the dynamic stress-strain diagram starting from zero stress indicates an increase of the bending modulus at low stress. Because of this behavior it is difficult to determine a definite dynamic proportional limit. The loading rate has a significant effect on the stress-strain behavior at all starting stresses. In general, the deformation at a given stress is increasing with decreasing loading rate.

For 2024-T4 aluminum alloy the stress-deformation curve under both static load and progressively increasing alternating load remains linear up to 43,000 psi. This stress is far beyond the fatigue strength of 27,000 psi at  $10^7$  cycles of this material. These results show that the dynamic proportional limit of 2024-T4 does not indicate the fatigue strength.

It is apparent from the above that even though Gough's dynamic proportional limit method may give a reliable indication of the fatigue strength of some materials, it may be misleading for many materials.

## SECTION IX. SUMMARY AND CONCLUSIONS

The purpose of the work was to investigate strength, damping and elasticity properties of various engineering alloys (SAE 1020 steel, 2024-T4 aluminum alloy, SAE 4340 steel, and RC-55 titanium) under progressively increasing stress amplitude, and to study the reliability of various short time fatigue testing methods using progressive load increase. Tests were performed under constant stress amplitude and under uniformly increasing stress amplitude starting from various stresses in the range from zero to the fatigue strength.

Tests under constant stress amplitude indicated that at low and intermediate stress amplitude the damping energy does not change with number of cycles, whereas when the stress amplitude exceeds a certain value, which is in general smaller than the fatigue strength, damping is a function of number of prior stress cycles. The stress which marks the beginning of stress history effects is called the cyclic stress sensitivity limit. One might expect that since there is no apparent change in damping below the cyclic stress sensitivity limit, correspondingly there might be little effect of cyclic stress below this limit on subsequent fatigue strength. Therefore in the progressive load increase work starting stresses both below and above this limit were used for some materials.

The following observations and conclusions may be made from the data presented for the materials tested:

1. Stress history below the cyclic stress sensitivity limit has relatively little effect on the fatigue strength properties. The magnitude of the starting stress is therefore insignificant as long as it is below the cyclic stress sensitivity limit. Starting stresses above this limit may result in significantly different failure stresses. RC-55 titanium may be an exception to this observation.

# Contrails

2. If the failure stresses obtained under progressive load increase are plotted versus the square root of the loading rate as suggested by Prot a curve rather than a straight line is generally observed. However, if a straight line is approximated through these points the fatigue strength so determined is, in all cases investigated, within  $\pm 10$  per cent of the conventionally determined fatigue strength.
3. If the Prot test data are plotted according to an exponent  $n_s$  of the loading rate which results in the straightest line the fatigue strength so determined may be considerably smaller than the conventionally determined fatigue strength.
4. According to Henry (6) the exponent  $n_m$  can also be determined from the conventional S-N curve. However, these values differ in most cases from the exponents determined by the two other methods and result in no improvement in indicating the conventional fatigue strength.
5. Lehr's damping intercept gives a fairly good indication of the fatigue strength of mild steel and titanium. However, Lehr's criterion is a rough approximation and neglects the stress history effect.
6. Gough's method which is based on the dynamic proportional limit gives a fair indication of the fatigue strength for steel. Since 2024-T4 aluminum alloy does not display a dynamic proportional limit in the stress range of interest, Gough's method is not suitable as Gough himself previously recognized. Since the dynamic proportional limit is a function of loading rate and increases with increasing loading rate these factors must be considered in using this method.
7. Lehr's and Gough's methods are probably an implication of the cyclic stress sensitivity limit. In general, the dynamic proportional limit and the change in slope of the damping curve occur at the cyclic stress sensitivity limit.
8. All short-time fatigue testing methods using progressive load increase have serious limitations. However, Prot's method or extensions thereof can be applied to a wider range of material types than the two other short-time testing methods investigated.
9. The titanium investigated in this work shows characteristics which differ in a few important respects from the other materials. However, the Prot approach appears to be reasonably reliable for this materials.

## BIBLIOGRAPHY

1. Vitovec, F. H. and Lazan, B. J., "Review of Previous Work on Short-Time Tests for Predicting Fatigue Properties of Materials," WADC TR 53-122, Wright Air Development Center, August 1953.
2. Prot, E. M., "L'Essai de Fatigue Sous Charge Progressive," Comptes Rendus, Vol. 225, pp. 667 (October 20, 1947).  
Prot, E. M., "L'Essai de Fatigue Sous Charge Progressive, une nouvelle technique d'essai de materiaux," Revue de Metallurgie, Vol. 45, pp. 481-489. (1948). English translation by E. J. Ward, "Fatigue Testing Under Progressive Loading; A New Technique for Testing Materials," WADC TR 52-148, Wright Air Development Center, September 1952.
3. Weibull, W., "Statistical Representation of Fatigue Failures in Solids," Kunigl. Techn. Hogsk. Handlingar No. 27, 1949.
4. Sinclair, G. M., "An Investigation of the Coaxing Effect in Fatigue of Metals," Proc. Am. Soc. Test. Mat., Vol. 52, pp. 743 (1952).
5. Richard, F. E. and Newmark, N. M., "A Hypothesis for the Determination of Cumulative Damage in Fatigue," Proc. Am. Soc. Test. Mat., Vol. 48, pp. 767-800 (1948)
6. Henry, D. L., "Prediction of Endurance Limits Using Linearly Increasing Loads," unpublished report, March 10, 1951.
7. Miner, M. A., "Cumulative Damage in Fatigue," Trans. Am. Soc. Mech. Eng., Vol. 67, pp. A159-A164 (1945).
8. Stulen, F. B. and Lamson, W. D., "Preliminary Report of the Progressive Load Method of Fatigue Testing," unpublished report, Curtiss-Wright Corp. Propeller Division, April 1951.
9. Ward, E. J. and Schwartz, D. C., "Investigation of Prot Accelerated Fatigue Test," WADC TR 52-234, Materials Laboratory, Wright Air Development Center, November 1952.
10. Boresi, A. P. and Dolan, T. J., "An Appraisal of the Prot Method of Fatigue Testing, Part I," Tech. Report 34, ONR Project NR-031-005, Theoretical and Applied Mechanics Department, University of Illinois, January 1953.  
Corten, H. T., Dimoff, T., Dolan, T. J., and Sugi, Masaki, "An Appraisal of the Prot Method of Fatigue Testing, Part II," Tech. Report 35, ONR Project NR-031-005, Theoretical and Applied Mechanics Department, University of Illinois, June 1953.
11. Corten, H. T., Dimoff, T., and Dolan, T. J., "An Appraisal of the Prot Method of Fatigue Testing," Proc. Am. Soc. Test. Mat., Vol. 54, Preprint No. 69 (1954).
12. Cummings, H. N., "Investigation of Materials Fatigue Problems Applicable to Propeller Design," Curtiss-Wright Corp., Propeller Division, Progress Report, No. 6, May 1954.
13. Gough, H. J., "The Fatigue of Metals," New York, D. Van Nostrand, pp. 244, 1926.
14. Lehr, E., "Die Abkürzungsverfahren zur Ermittlung der Schwingungsfestigkeit von Materialien," Doktor-Ing. Dissertation, Stuttgart, 1925.
15. Lazan, B. J., "Fatigue Failure Under Resonant Vibration Conditions," Fatigue. Am. Soc. for Metals, Cleveland 1954, pp. 36-76.



16. Lazan, B. J., "A Study with New Equipment of the Effects of Fatigue Stress on the Damping Capacity and Elasticity of Mild Steel," Proc. Am. Soc. Metals, Vol.4, pp.499-599 (1950).
17. Vitovec, F and Slibar, A, "Ueber den Einfluss der freien Oberflache auf die Verformungsbehinderung im vielkristallinen Werkstoff. Schweizer Arch. 16 (1950) pp. 76-80.

Vitovec, F. H., "The Effect of Specimen Surface as a Discontinuity in Fatigue Phenomena, WADC TR 53-167, Wright Air Development Center, September 1953.

TABLE I - TEST MATERIALS AND DATA

Material	2024-T4		RC-55 Titanium
	SAE 1020 Steel	Aluminum Alloy	
Source	Crucible Steel Company	Aluminum Company of America	Rem-Cru Titanium
Chemical Composition	0.2 C, 0.45 Mn 0.45 P, 0.055S Bal. Fe.	4.20 Cu, 1.66 Mg 0.63 Mn, 0.30 Fe 0.14 Si, 0.07 Zn, 0.02 Cr, 0.02 Ti Bal. Al.	0.045 C, 0.067 N 0.075 O, 0.0044 H Bal. Ti.
Received as	Hot-rolled	Hot-rolled, drawn and aged.	Hot-rolled, annealed.
Treatment after Receipt			Forged at 1700-1800 F. Hot rolled at 1450-1550 F. Annealed 1 hr. at 1300 F.
Modulus of Elasticity psi	$29.4 \times 10^6$	$10.6 \times 10^6$	$16.4 \times 10^6$
Yield Strength psi	42,000	48,600	57,000
Tensile Strength psi	69,000	72,800	75,000
Elongation %	30	21.4	24.5
Reduction of Area %	60.5		25
Hardness	$R_B = 90$	$R_A = 48.5$	$R_B = 88$
Specimen Diameter inch	0.375	0.585	0.25
Fatigue Strength thousands of psi	35.0	27.0	43.0
Loading Rates psi per cycle	0.0025 0.0250 0.0900	0.009 0.027 0.076	0.01 0.04 0.09
Starting stresses psi	0 29,000 33,000 37,000	0 24,000	0 23,000 34,000 41,000

Cyclic annealing: 1 hr., 1575 F. quench to 1225F, hold for 16 hrs., furnace to 1100 F, Air. Double normalizing: 1-1/2 hrs. 1650 F, air. 1 hr. 1650 F, air. Quench: Austenizing 1 hr. 1440 F, oil quench to 200 F. Temper: 1 hr. 1054 F, Air.

Contrails

TABLE II  
FATIGUE TEST DATA FOR SAE 1020 STEEL AT VARIOUS  
LOADING RATES AND DIFFERENT INITIAL STRESSES

Specimen Number A----L	Failure Stress KSI	Number of Cycles Kilocycles	Loading Rate PSI/Cycle	
2612	53.37	26.00	0	
2595	44.98	197.33	0	
2594	40.02	521.27	0	
2600	37.04	1,210.76	0	
2591	34.97	30,765.41	0	T.S.

STARTING STRESS 0 KSI

2579	52.99	550.14	0.09632	
2584	51.99	552.64	0.09408	
2577	47.71	1,634.75	0.02919	
2583	46.10	1,908.92	0.02415	
2582	42.87	17,983.60	0.002384	
2580	41.12	16,063.69	0.002560	

STARTING STRESS 29 KSI

2593	52.80	263.15	0.90956	
2586	52.61	260.55	0.90951	
2585	52.97	254.32	0.08994	
2588	46.62	761.48	0.02258	
2587	46.23	753.18	0.02230	
2589	46.06	751.95	0.02255	
2575	41.57	4,871.42	0.002590	
2576	41.06	4,484.50	0.002687	
2590	40.41	5,320.00	0.002155	

Specimen Aged After Polishing

2597	51.92	225.34	0.1015	
2598	46.17	682.22	0.02511	
2599	41.09	3,855.02	0.003130	

Specimen Stress Relief Annealed

2592	53.73	258.58	0.09568	
2581	44.94	711.04	0.02240	
2578	38.97	4,474.46	0.002227	

\_\_\_\_\_  
T. S. - Test stopped.

TABLE II (Cont.)

Specimen Number A----L	Failure Stress KSI	Number of Cycles Kilocycles	Loading Rate PSI/Cycle
STARTING STRESS 33 KSI			
2607	41.23	181.83	0.1003
2608	50.69	175.55	0.1008
2609	50.06	170.48	0.1001
2603	45.14	386.79	0.02495
2604	44.69	463.81	0.02515
2605	44.01	433.87	0.02536
2601	40.67	4,241.65	0.001809
2606	40.13	1,569.18	0.004557
2602	39.24	1,653.23	0.003772
STARTING STRESS 37 KSI			
2618	49.82	131.01	0.09830
2617	49.76	133.62	0.09610
2616	43.76	278.60	0.02443
2615	43.72	278.95	0.02462
2614	38.51	643.01	0.002538
2613	38.44	638.59	0.002548

TABLE III

FATIGUE TEST DATA FOR 2024-T4 ALUMINUM ALLOY AT VARIOUS  
LOADING RATES AND DIFFERENT INITIAL STRESSES

Specimen Number P----D	Failure Stress KSI	Number of Cycles Kilocycles	Loading Rate PSI/Cycle
1120	50.00	14.00	0
422	44.90	46.10	0
420	42.00	79.34	0
418	38.90	76.02	0
423	36.90	128.85	0
416	35.20	206.30	0
1128	33.00	170.38	0
1126	32.40	465.16	0
417	30.70	412.03	0
1134	28.00	9,466.63	0
456	26.04	13,543.46	0

STARTING STRESS 0 KSI

1117	44.80	500.00	0.0900
1122	43.60	517.60	0.0840
1121	39.80	1,322.00	0.0300
1130	38.40	1,291.00	0.0297
1115	38.40	1,313.00	0.0290
1118	36.50	3,763.00	0.00970
1119	33.20	11,592.00	0.00286

STARTING STRESS 24 KSI

1133	44.60	268.00	0.0768
1123	44.40	267.00	0.0764
1132	39.00	543.00	0.0276
1124	38.70	545.70	0.0270
1127	35.00	1,225.00	0.0090

TABLE IV

FATIGUE TEST DATA FOR SAE 4340 STEEL AT VARIOUS LOADING RATES

Specimen Number AH---L	Failure Stress KSI	Number of Cycles Kilocycles	Loading Rate PSI/Cycle
2224	120.17	19.42	0
2223	101.11	78.11	0
2222	88.55	113.86	0
2231	85.62	76.23	0
2220	82.36	131.14	0
2225	79.40	289.06	0
2227	75.13	168.20	0
2226	69.94	5, 579.04	0
2249	66.95	16, 749.12	0
2248	75.95	32, 341.92	0.002348
2247	72.60	30, 186.65	0.002405
2244	71.03	29, 909.80	0.002375
2237	67.00	28, 951.71	0.002314
2251	65.37	25, 691.02	0.002545
2257	62.56	26, 043.17	0.002402
2256	61.04	21, 496.25	0.002840
2255	59.97	24, 100.32	0.002488
2232	66.48	8, 231.23	0.008077
2241	66.02	8, 268.46	0.007985
2239	75.10	1, 842.56	0.04076
2245	81.15	3, 125.82	0.02596
2236	79.20	2, 370.68	0.03340
2235	77.33	3, 023.88	0.02557
2240	77.26	2, 324.20	0.03324
2234	70.78	2, 717.69	0.02605
2250	68.64	2, 642.33	0.02598
2252	67.37	2, 516.78	0.02677
2233	64.69	2, 671.62	0.02422
2246	100.03	1, 046.03	0.09563
2243	92.55	991.48	0.90335
2230	85.92	861.27	0.90076
2229	84.40	849.32	0.90040
2228	82.10	804.49	0.10200
2242	81.52	879.20	0.09272
2238	77.56	779.48	0.90050
2253	76.16	771.97	0.09866
2554	74.43	707.19	0.10520

FATIGUE TEST DATA FOR RC55 TITANIUM AT VARIOUS  
LOADING RATES AND DIFFERENT INITIAL STRESSES

Specimen Number AK---AA	Failure Stress KSI	Number of Cycles Kilocycles	Loading Rate PSI/Cycle
2402	50.00	12.33	0
2439	47.04	21.19	0
2443	43.50	180.22	0
2403	43.60	20, 250.00	0 T. S.
2404	40.61	20, 990.00	0 T. S.

STARTING STRESS 0 KSI

3891	52.16	564.83	0.09235
3881	51.65	488.32	0.10580
3878	50.76	489.07	0.10380
3866	51.34	1, 384.33	0.03713
3894	50.45	1, 130.40	0.04463
3892	48.78	1, 080.76	0.04513
3877	46.68	4, 094.60	0.01140
3893	44.98	4, 367.72	0.01030
3890	43.01	4, 221.90	0.01019

STARTING STRESS 23 KSI

3873	54.72	293.33	0.1077
3872	53.90	280.30	0.1102
3864	53.35	252.99	0.1195
3875	49.75	567.97	0.04705
3874	49.09	527.33	0.04905
3867	49.09	648.30	0.03828
3876	46.36	2, 359.93	0.009915
3880	45.64	1, 725.67	0.013100
3870	43.84	2, 205.54	0.009426
3865	43.37	2, 526.81	0.008281

STARTING STRESS 34 KSI

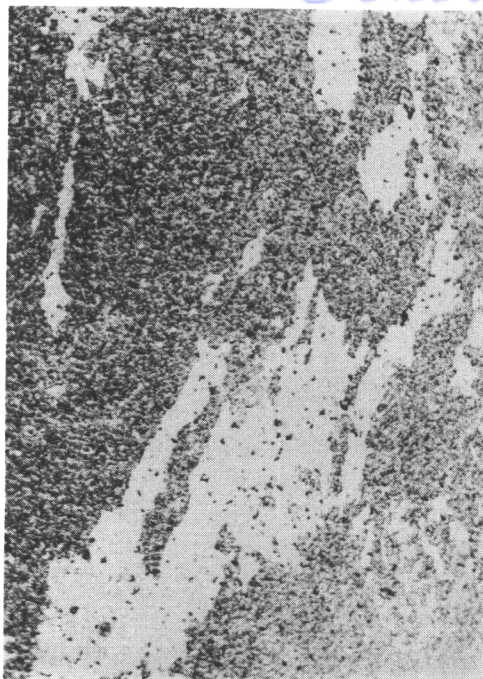
3879	51.33	166.94	0.1048
3888	50.82	168.74	0.0987
3889	50.12	163.03	0.0977
3886	48.93	325.87	0.04539
3885	48.46	319.35	0.04488
3882	47.90	292.17	0.04713
3884	47.03	1, 157.75	0.01116
3883	45.12	1, 092.64	0.01013
3887	43.81	993.66	0.01031

T. S. - Test stopped.

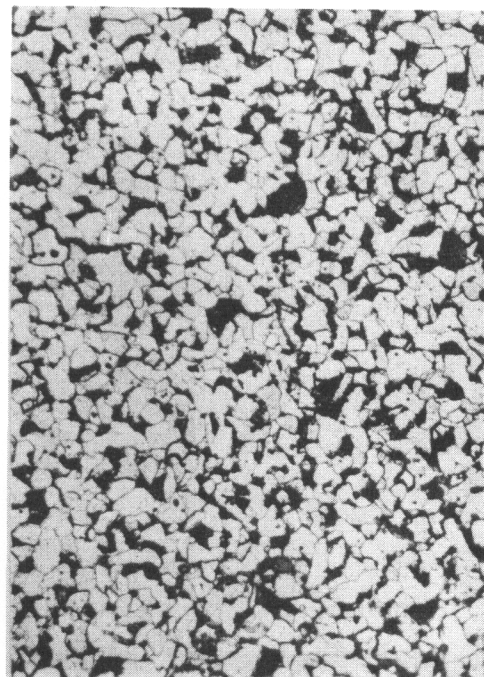
TABLE V (Cont.)

Specimen Number AK-----AA	Failure Stress KSI	Number of Cycles Kilocycles	Loading Rate PSI/Cycle
STARTING STRESS 41 KSI			
3902	52.47	118.27	0.09797
3901	52.42	115.25	0.09976
3899	50.66	197.86	0.04933
3900	50.52	198.86	0.04841
3897	46.84	605.08	0.01025
3898	46.48	451.92	0.01272

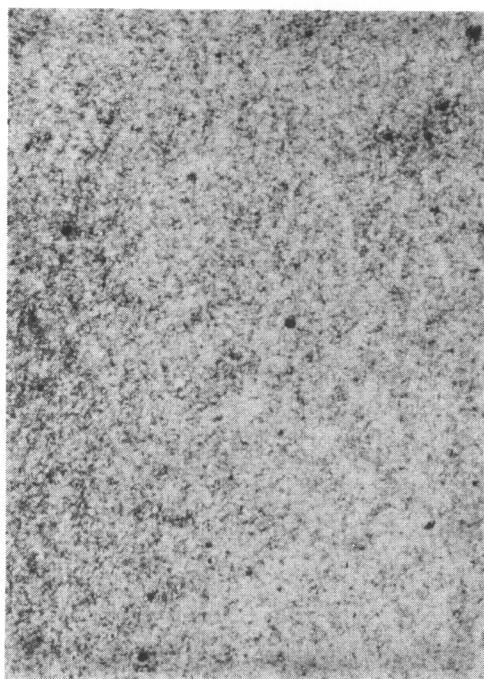




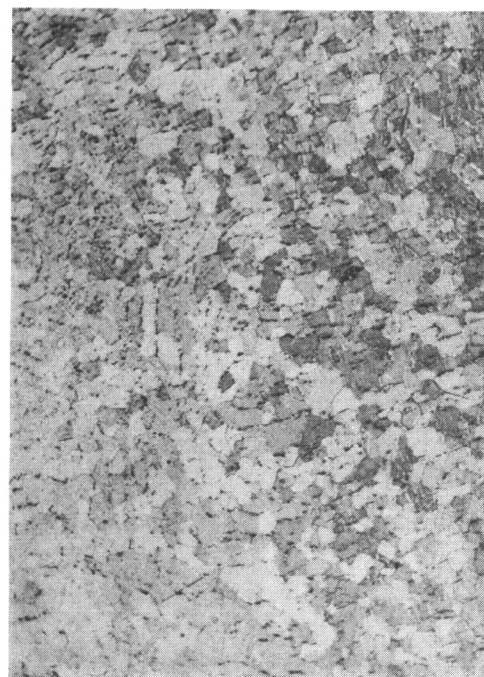
100X Trans. Keller's Etchant  
24S-T4



100X 5% Nital Etchant  
SAE 1020



100X 3% Picral Etchant  
SAE 4340



100X 5HNO<sub>3</sub>, 1 HF, 94 H<sub>2</sub>O  
RC-55 Titanium

Fig. 1. - Photomicrographs of Test Materials in Testing Condition.



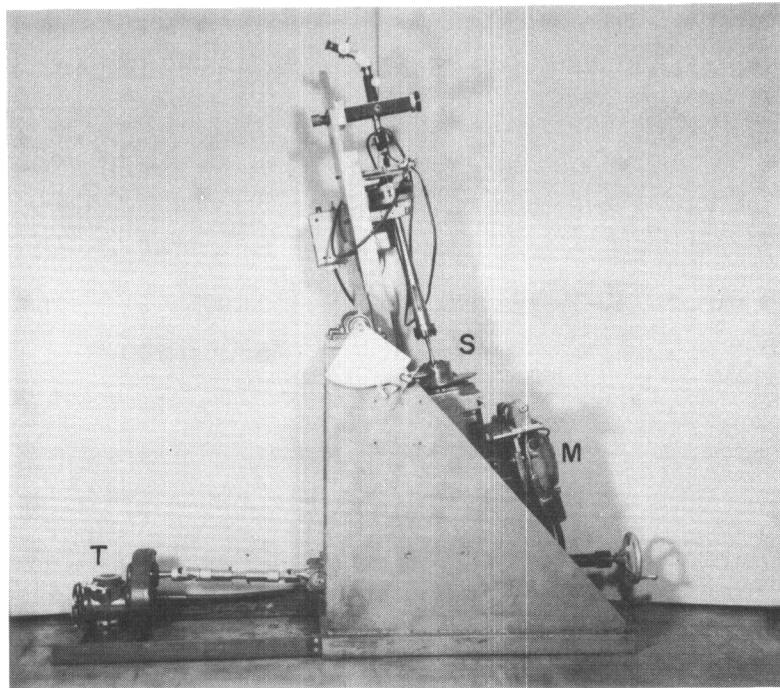


Fig. 2. - Rotating Cantilever Beam Fatigue and Damping Testing Machine with Variable Speed Transmission for Progressive Load Increase Tests.

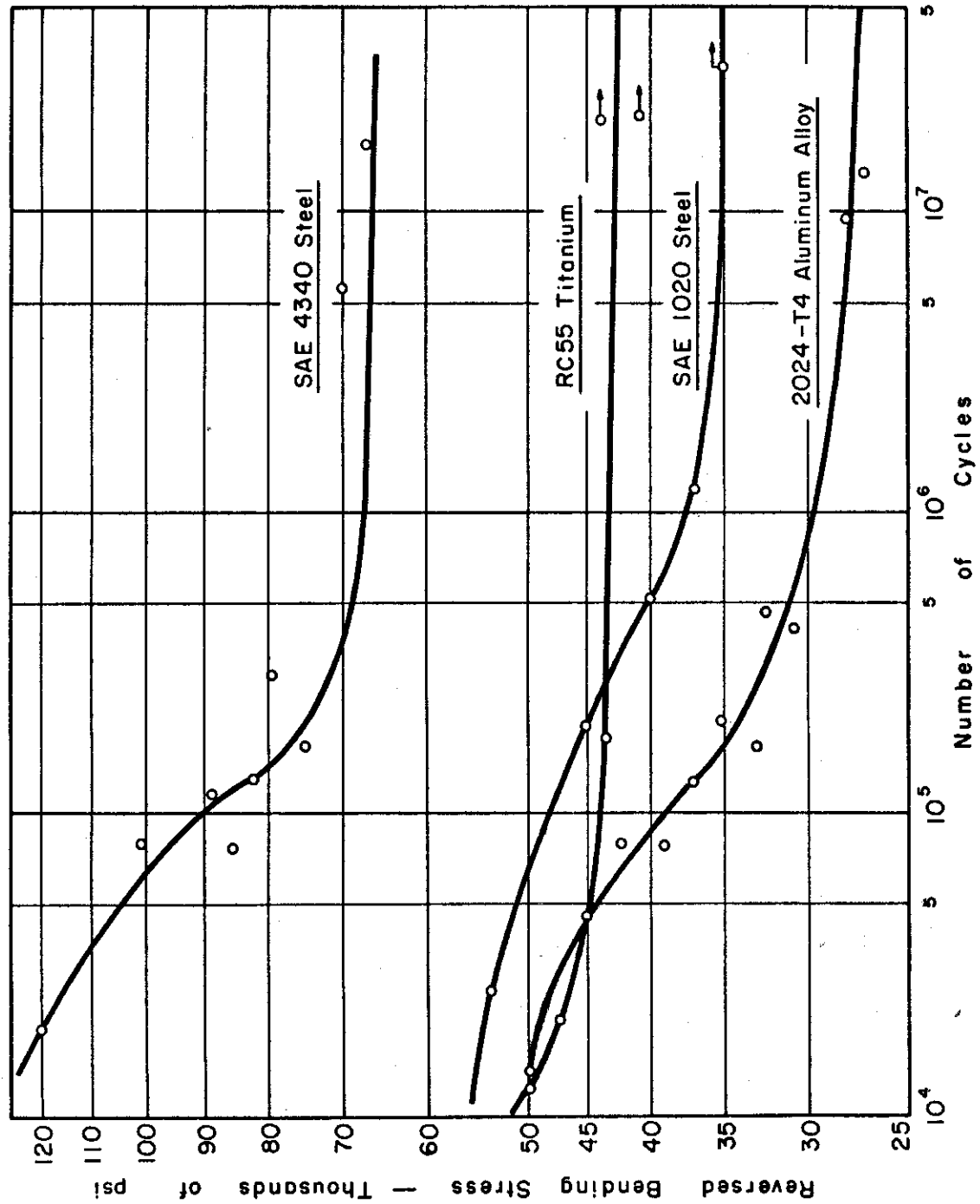


Fig. 3 S-N Fatigue Diagrams of Test Materials.

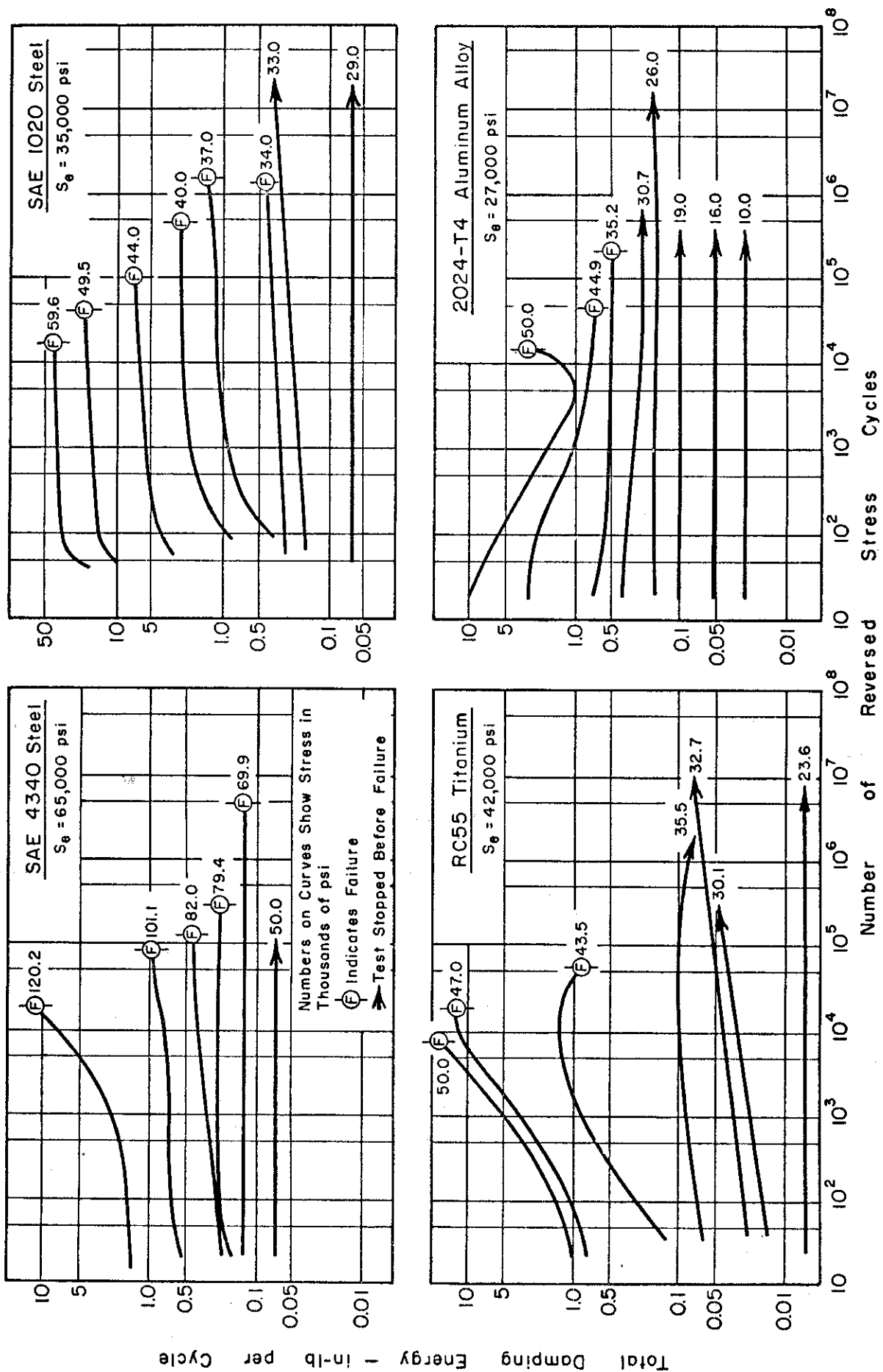


Fig. 4 Comparison of the Effect of Cyclic Stress of Several Magnitudes on the Total Damping Energy of Test Materials.

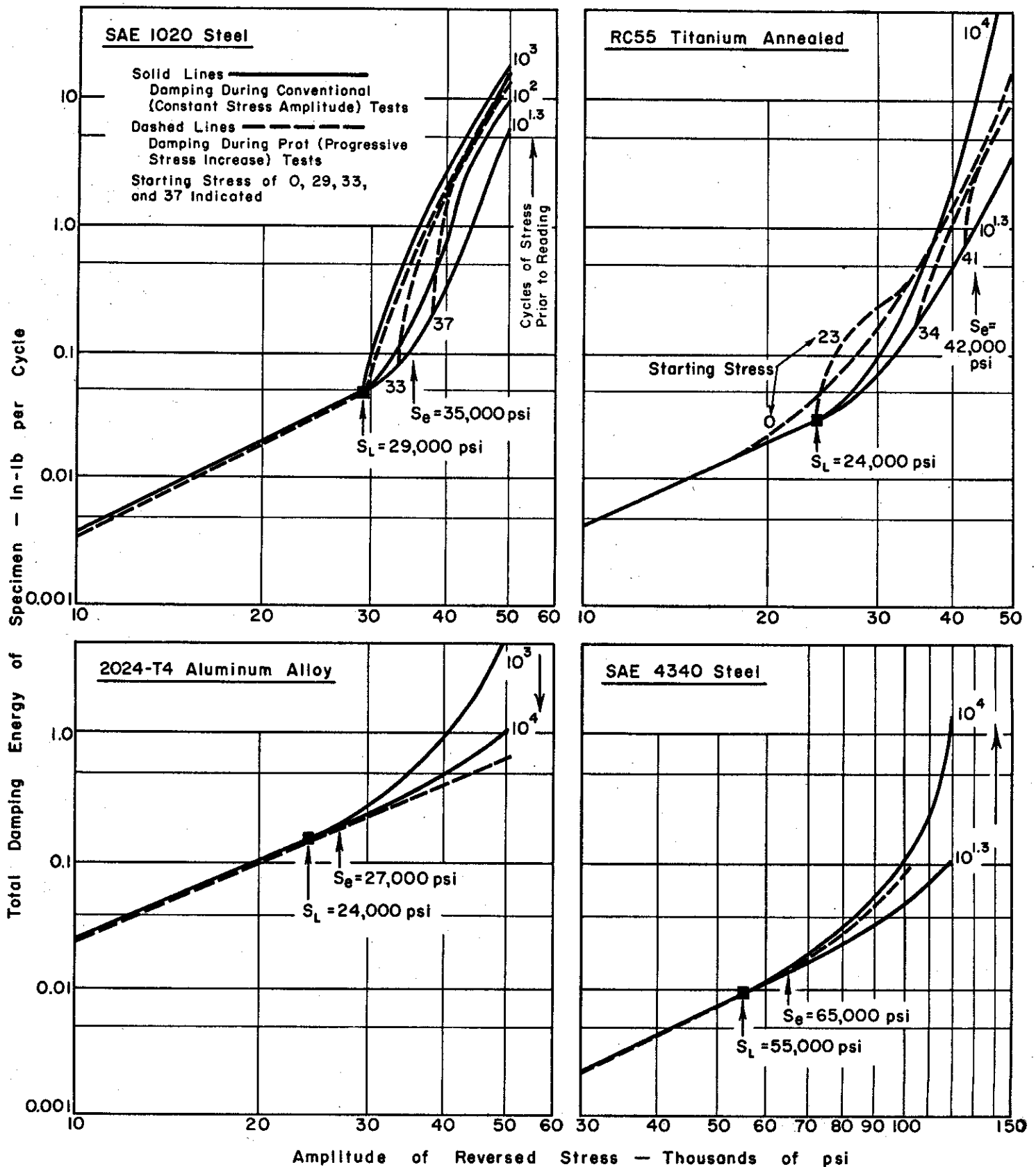


Fig.5 Total Damping Energy of Test Specimen Under Both Constant and Progressively Increasing Stress Amplitude as a Function of Stress for Various Stress Histories.

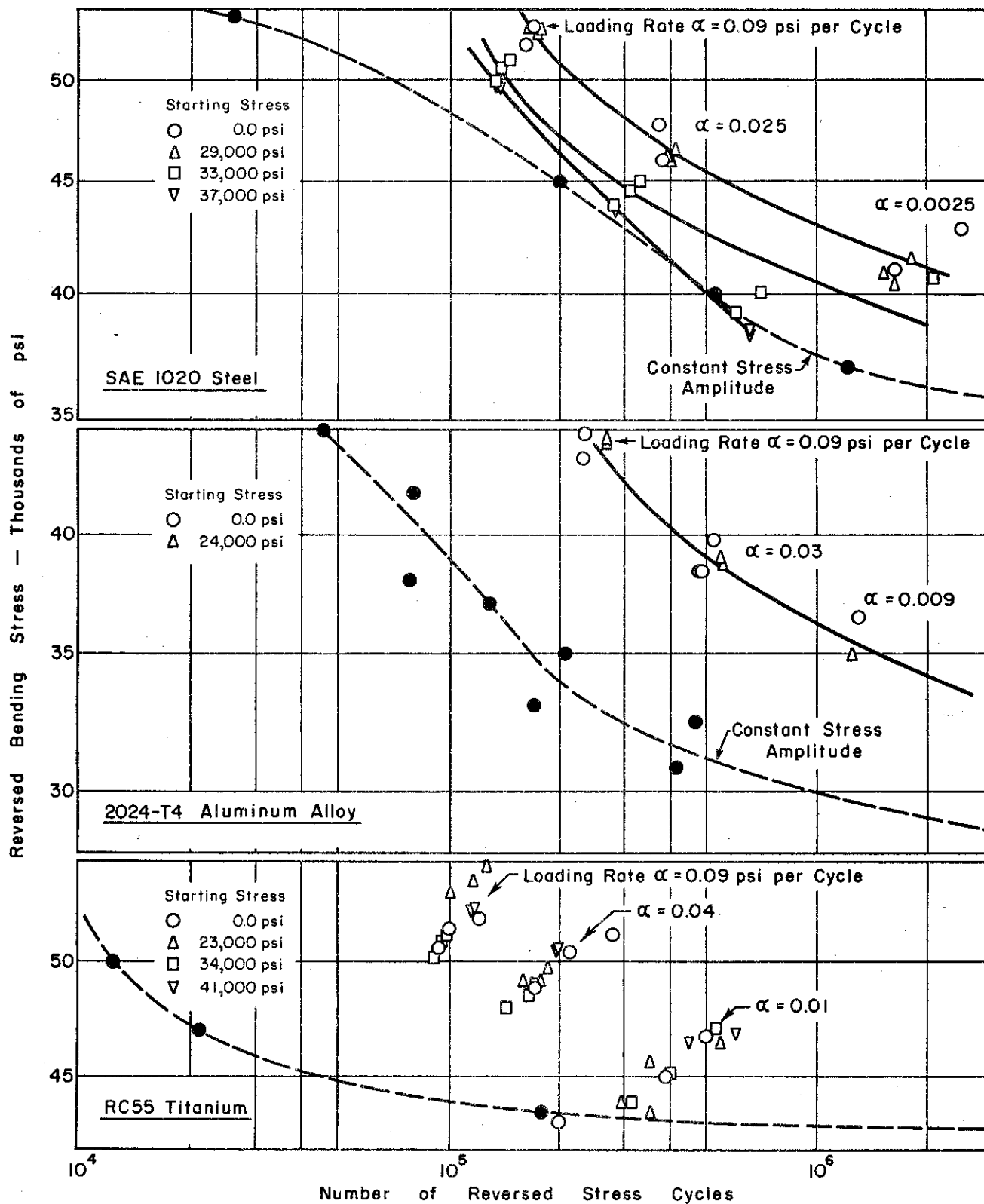


Fig. 6 S-N Curves Obtained Under (a) Constant Stress Amplitude Conventional Tests and (b) Uniformly Increasing Stress Amplitude. Cycles Plotted are Those Above Highest Starting Stress.

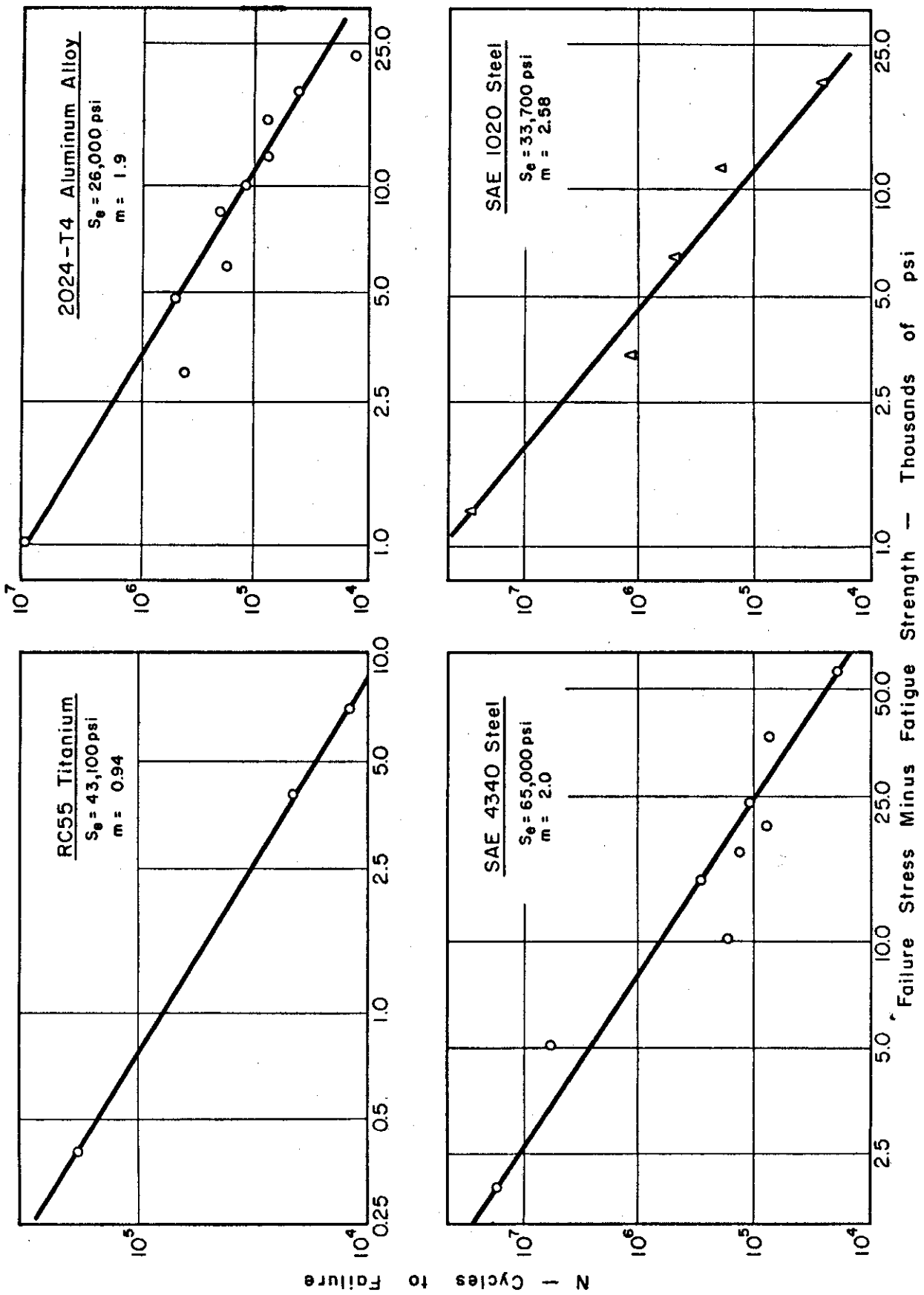


Fig. 7  $N$  Versus  $(S - S_e)$  Diagram for Determination of the Constants in Weibul's Equation.

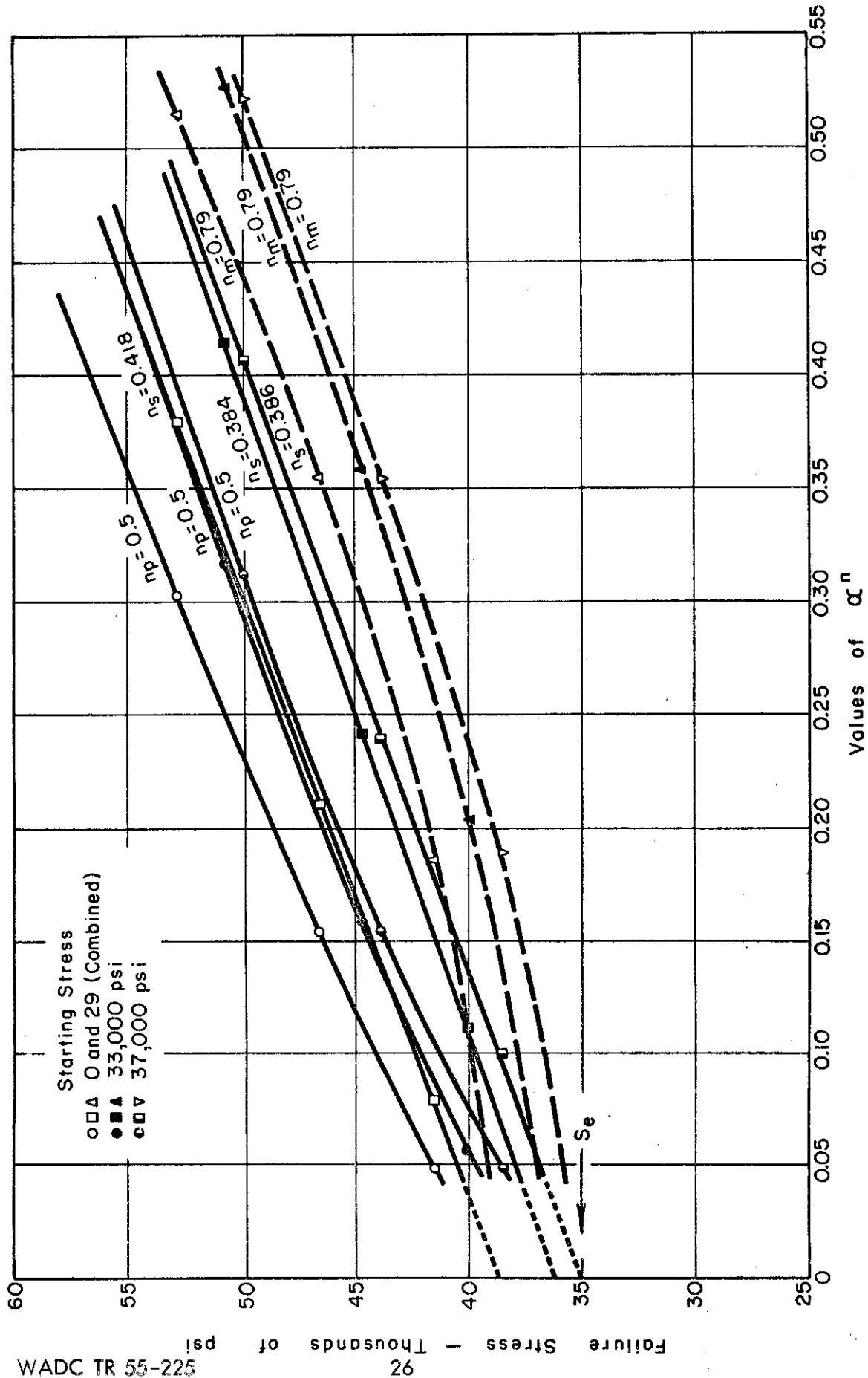


Fig. 8 Failure Stress Under Progressive Load Increase as a Function of Loading Rate  $\alpha$  to the Various Values of Power  $n$  for SAE 1020 Steel.



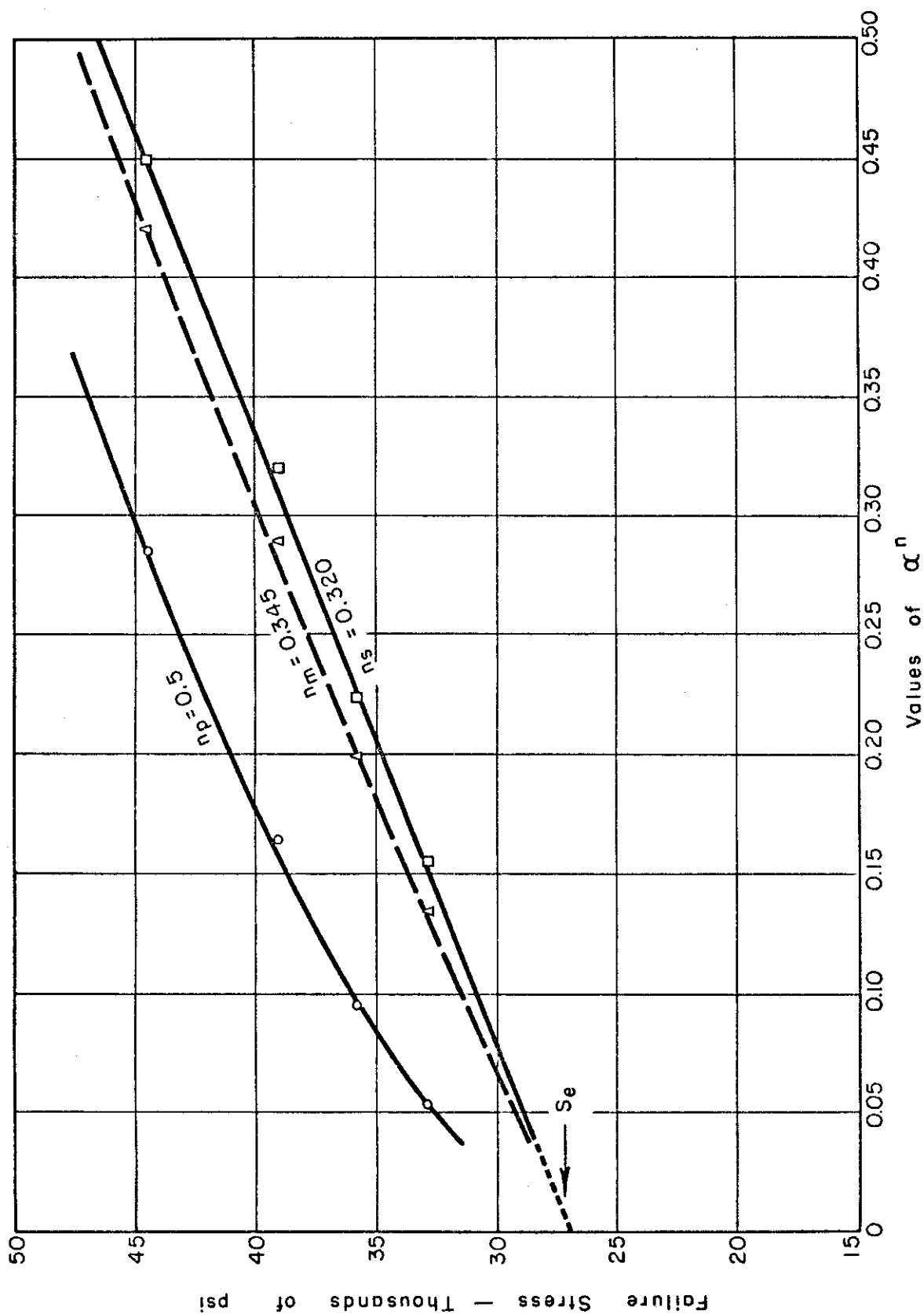


Fig. 9 Failure Stress Under Progressive Load Increase as a Function of Loading Rate  $\alpha$  to the Various Values of Power  $n$  for 2024-T4 Aluminum Alloy.

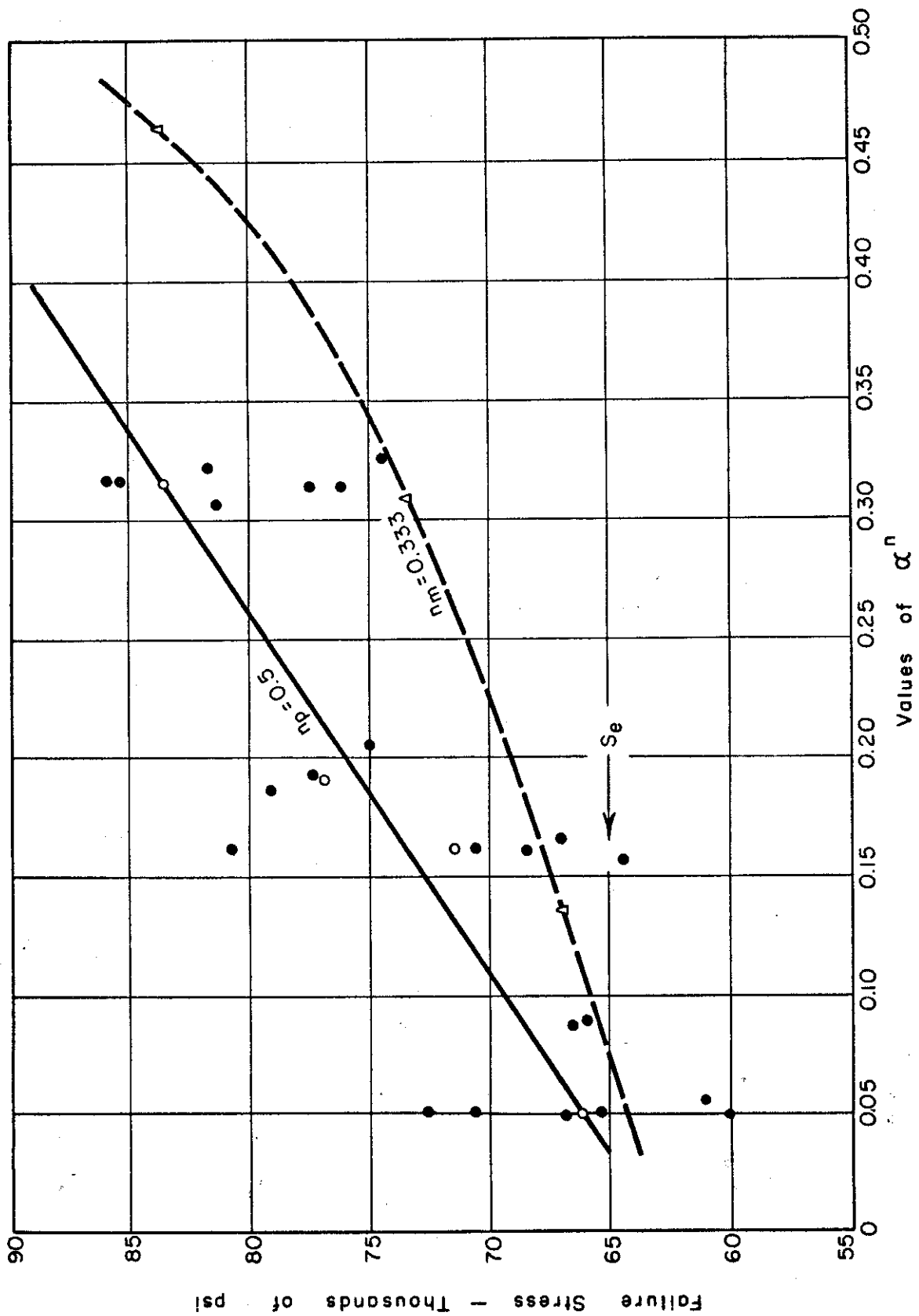


Fig. 10 Failure Stress Under Progressive Load Increase as a Function of Loading Rate  $\alpha$  to the Various Values of Power  $n$  for SAE 4340 Steel.

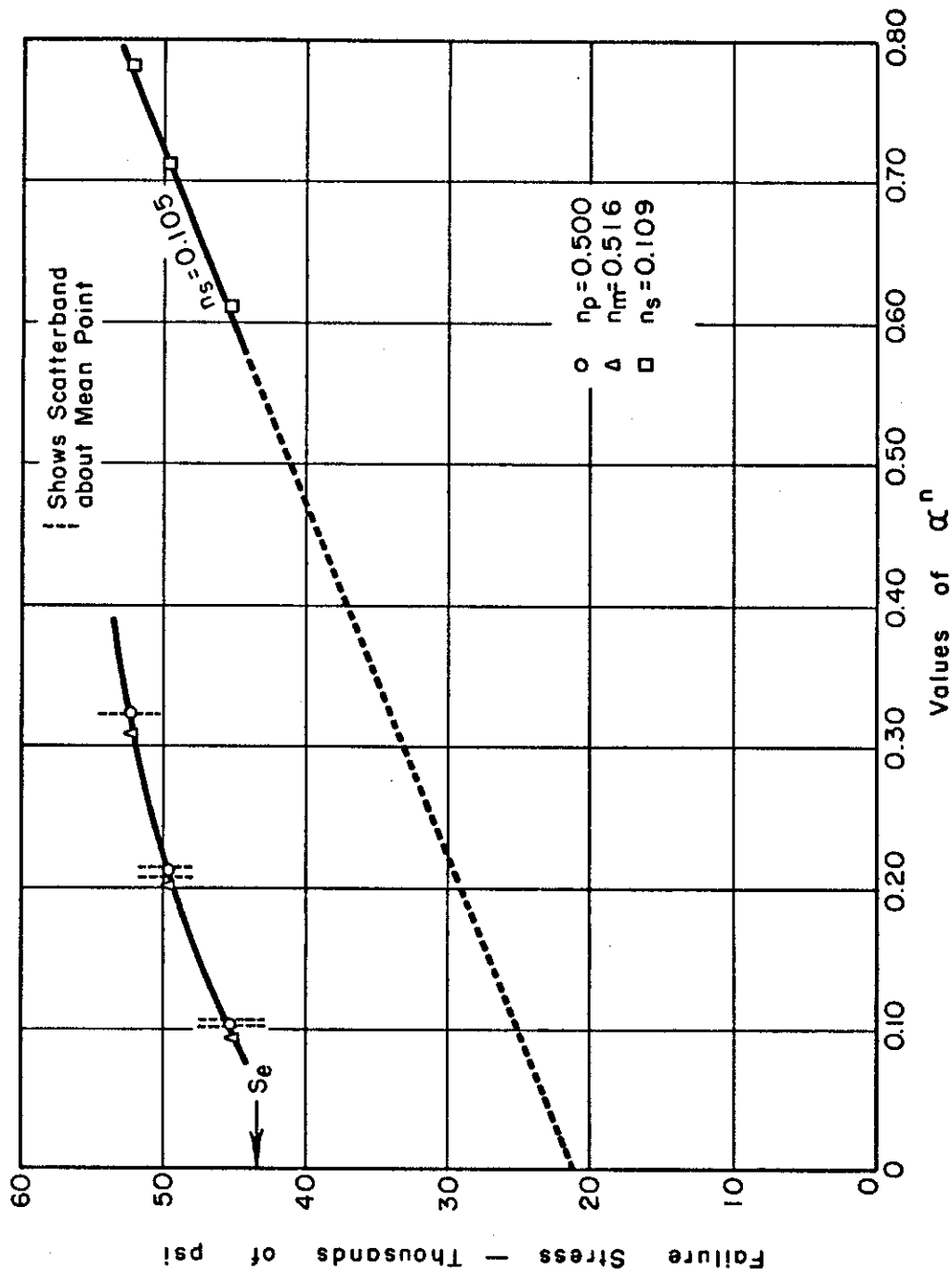


Fig. 11 Failure Stress Under Progressive Load Increase as a Function of Loading Rate  $\alpha$  to the Various Values of Power  $n$  for RC55 Titanium.

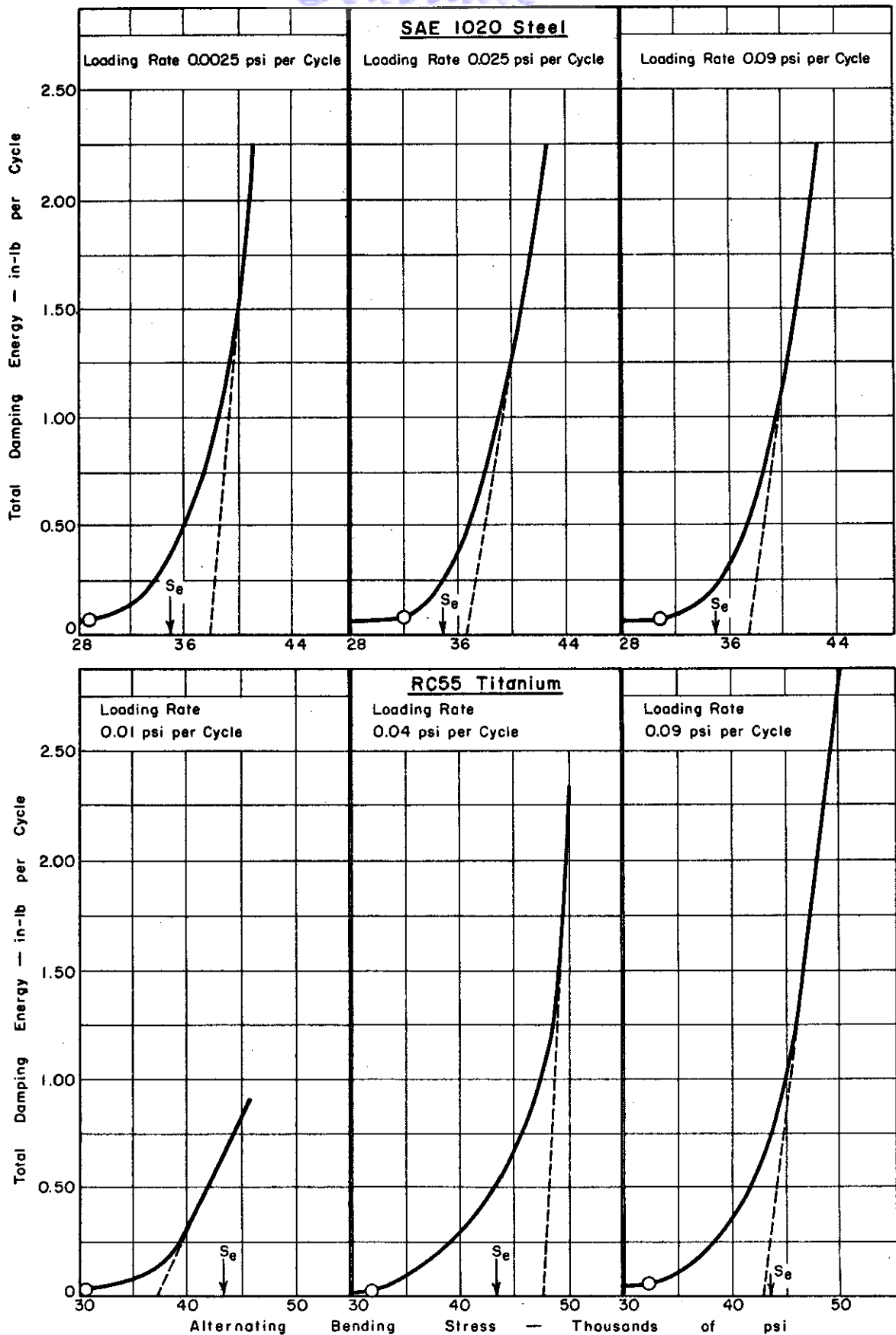


Fig.12 Linear Plot of Damping Energy Versus Alternating Stress at Different Loading Rates for SAE 1020 Steel and RC55 Titanium.

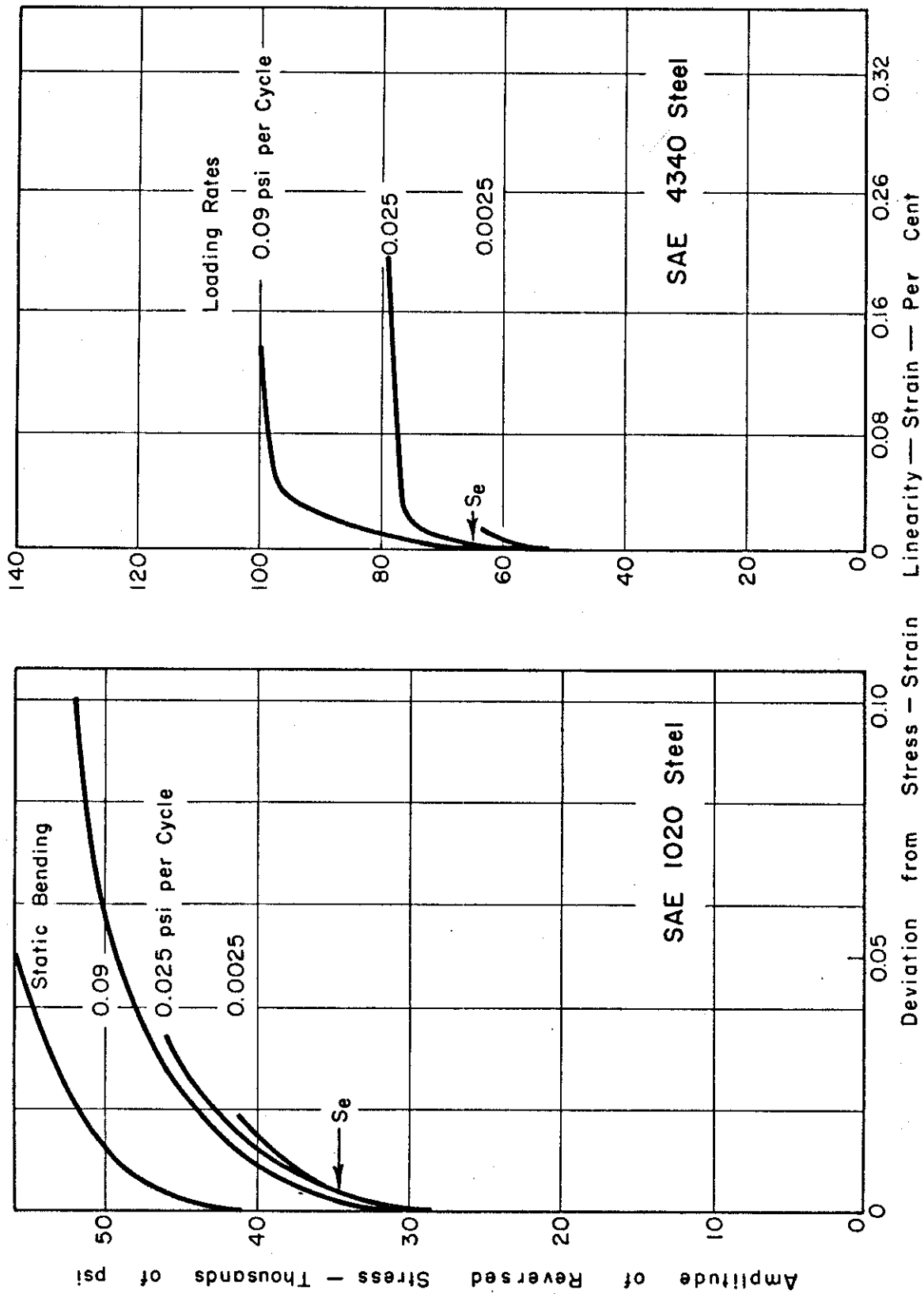


Fig.13 Deviation from Stress-Strain Linearity as a Function of Amplitude of Reversed Stress and Various Loading Rates for SAE 1020 and SAE 4340 Steel.

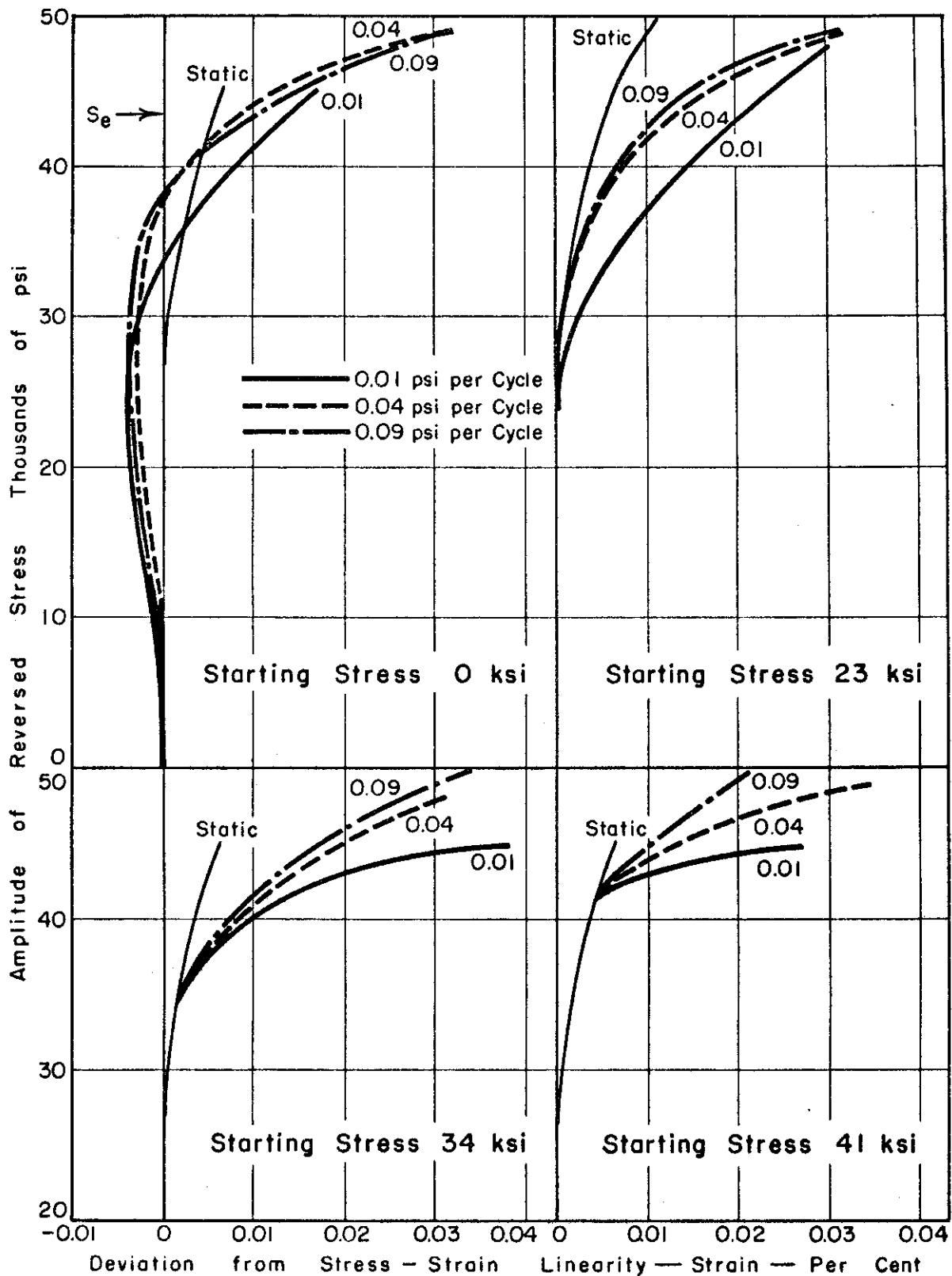


Fig.14 Deviation from Stress-Strain Linearity as a Function of Amplitude of Reversed Stress, Loading Rate, and Starting Stress for RC55 Titanium.